HD-THEP-94-31

The Strongly Interacting Electroweak Phase Transition

B.Bergerhoff[1] and C.Wetterich[2]

Institut für Theoretische Physik
Universität Heidelberg
Philosophenweg 16, D-69120 Heidelberg

Abstract

A quantitative discussion of nonperturbative effects for the high temperature electroweak phase transition is presented. We propose a method for the computation of the temperature dependent effective scalar potential that takes into account the running of the effective gauge coupling. Compared to perturbation theory we find a moderate decrease of the critical temperature and an important change in the strength of the first order transition. We conclude that perturbation theory gives a misleading picture of the dynamics of the transition.

[1] e-mail: et8@ix.urz.uni-heidelberg.de
[2] e-mail: wetteric@post.thphys.uni-heidelberg.de

1 Introduction

It has recently been suggested ([1] - [4]) that the electroweak high temperature phase transition may be governed by a strongly interacting gauge theory. The associated nonperturbative phenomena are believed to play only a modest role if the mass of the Higgs scalar is very small. For realistic mass values consistent with the experimental lower bounds [5], however, the nonperturbative effects could dominate the quantitative and perhaps even qualitative behaviour of the high temperature effective potential for the Higgs scalar. If so, this will have important consequences for speculations [6] that the observed baryon asymmetry might have been created during the electroweak phase transition in the early universe. Baryon generation within the standard model not only requires substantial CP violation but also a sufficiently strong first order phase transition. This is necessary in order to guarantee a period in the evolution of the early universe where baryon number violating processes are out of thermal equilibrium. The order of the electroweak phase transition as well as many important details of its cosmological dynamics are encoded in the shape of the high temperature effective potential. This has recently been studied using different versions of resummed perturbation theory [7]. Sizable deviations from the perturbative results change the rates of baryon number violating processes or bubble formation by many orders of magnitude and can therefore completely alter our picture of the phase transition.

The importance of nonperturbative electroweak physics was first observed quantitatively [8] in a simplified theory where all particles except for the Higgs scalar were neglected. In contrast to the perturbatively suggested [9] weak first order behaviour, the phase transition of this model was found to be of the second order, with critical exponents corresponding to the universality class of the three dimensional model. Near the transition the dimensionless couplings are strong (as dictated by the values of corresponding infrared fixpoints [10]) and perturbation theory becomes inadequate. More generally, at nonvanishing temperature T the physics of the modes with momenta $q^2 < (2\pi T)^2$ can always be described by an effective three dimensional theory [11]. The crucial question is to what extent the fluctuations of these low momentum modes dominate the behaviour of the effective potential. In the pure scalar theory an investigation of the scale dependence of the effective average potential revealed that the running of the couplings becomes effectively three dimensional ([8], [12]) for scales below $2\pi T$, but the difference between the three- and the four-dimensional running has quantitatively important effects only in a narrow temperature range around the critical temperature where the dimensionless quartic scalar coupling becomes strong.

In the electroweak standard model one expects even stronger nonperturbative effects. In the effective three dimensional theory at scales below $2\pi T$ the running of the gauge coupling is not logarithmic as in four dimensions, but gouverned by a power law [1]. In consequence, the three dimensional "confinement scale"

was estimated between $T/10$ and $T/5$ [1]. This scale is characteristic for the nonperturbative effects generated by the strong gauge coupling and determines, for example, the magnitude of W-boson condensates in complete analogy to QCD. In this work we give a more quantitative estimate of the modifications of the high temperature effective potential due to the three dimensional running of couplings. We will perform a "renormalization group improvement" for the scalar potential $U(\varphi)$ in the effective three dimensional theory which is in spirit very similar to the "renormalization group improved one loop potential" proposed for the zero temperature case by Coleman and Weinberg [13]. This approach accounts properly for the three dimensional running of the effective couplings and is expected to be quantitatively very reliable as long as the φ-dependent gauge boson masses are sufficiently large compared to the confinement scale. This gives, in turn, a lower bound on the value of the scalar field $|\varphi|$ for which the potential $U(\varphi)$ is quantitatively under control. For $|\varphi|$ smaller than this lower bound nonperturbative effects are expected to give important modifications. We will give rough estimates of the size of these effects and demonstrate that nonperturbative physics dominates the phase transition for realistic values of the mass of the Higgs scalar.

The three dimensional physics is related to the infrared behaviour of the theory. Perturbation theory is plagued by strong infrared divergences in the presence of massless particles as the gauge bosons for $\varphi = 0$. A suitable method to deal with these difficulties is the average action Γ_k [14] where an effective infrared cutoff k controls the infrared behaviour. The dependence of Γ_k on the scale k is governed by an exact nonperturbative flow equation [15]. For nonzero temperature this flow equation accounts properly for the change from an effective four dimensional running of couplings for $k^2 > (2\pi T)^2$ to the three dimensional running for $k^2 < (2\pi T)^2$ [8]. We use here a simplified description by a pure three dimensional theory for $k < k_T$, $k_T = 2\pi T$. The "initial value" of Γ_{k_T} includes the effects of all quantum fluctuations except those of the modes of the three dimensional theory with $q^2 < k_T^2$. It is obtained by integrating out the $n \neq 0$ Matsubara frequencies, the high momentum modes of the $n = 0$ frequency and all modes of the zero components of the gauge fields A_0. In particular we are interested in the average potential U_k and we can infer the shape of U_{k_T} from the work of reference [16] (see below). For $k \to 0$ the average potential becomes exactly the high temperature effective potential ([8],[15]). The latter can therefore be computed by solving the flow equation for k between k_T and 0. As a further simplification we leave out the fermions and the hypercharge gauge field.

2 Nonperturbative flow equation

Approximate solutions of the exact flow equation need a truncation of the most general form of Γ_k and we will work with the ansatz

$$\Gamma_k\left[\varphi, A_\mu\right] = \int d^dx \left(U_k(\rho) + Z_{\varphi,k}|D_\mu\varphi|^2 + \frac{1}{4}Z_{F,k}F_{\mu\nu}F^{\mu\nu}\right). \tag{1}$$

Here $\rho = \varphi^\dagger\varphi$ and group indices are omitted. The form of the average potential $U_k(\rho)$ is left arbitrary and has to be determined by solving the flow equation. For the Abelian Higgs model the evolution equation for the average potential was computed in the approximation (1) in reference [17]. Inserting the appropriate $SU(2)$ group factors we obtain in the Landau gauge ($\alpha = 0$), with $t = \ln k$

$$\begin{aligned}\frac{\partial}{\partial t}U_k(\rho) &= \frac{1}{2}\int\frac{d^dq}{(2\pi)^d}\frac{\partial}{\partial t}\left(3\,(d-1)\ln\left(q^2+k^2+m_B^2\right)+\right.\\ &\left.+\ln\left(q^2+k^2+m_1^2\right)+3\ln\left(q^2+k^2+m_2^2\right)\right)\end{aligned} \tag{2}$$

where the mass terms read

$$m_B^2 = \frac{1}{2}Z_{\varphi,k}\bar{g}^2\rho\ ;\ m_1^2 = \left(U_k'(\rho)+2\rho U_k''(\rho)\right)/Z_{\varphi,k}\ ;\ m_2^2 = U_k'(\rho)/Z_{\varphi,k}. \tag{3}$$

We have used here a masslike infrared cutoff $R_k = Z_k k^2$ but more general cutoff functions $R_k(q)$ may be employed. The partial derivative $\frac{\partial}{\partial t}$ on the right hand side of (2) is meant to act only on R_k and we omit contributions arising from the wave function renormalization Z_k in R_k. Primes denote derivatives with respect to ρ.

This flow equation can be used[1] in arbitrary dimensions d and constitutes a nonlinear partial differential equation for the dependence of U on the two variables k and ρ. In our case it holds for the three dimensional potential U_3 and a correspondingly normalized scalar field ρ_3. They are related to the usual four dimensional quantities by $U_3 = U_4/T$, $\rho_3 = \rho_4/T$. The gauge coupling in (3) stands for the three dimensional running renormalized gauge coupling $\bar{g}_3^2(k)$. Its value at the scale k_T is given by

$$\bar{g}_3^2(k_T) = g_4^2(k_T)T\left(1-\frac{g_4^2(k_T)T}{24\pi m_D}\right) \tag{4}$$

where

$$m_D^2 = \frac{5}{6}g_4^2(k_T)T^2 \tag{5}$$

[1] The ultraviolet divergence on the right hand side of equation (2) is particular to the use of a masslike infrared cutoff. For $d < 4$ it concerns only an irrelevant constant in U and is absent for $\partial U'/\partial t$.

and the effects of integrating out the A_0 mode have been included in lowest order [16]. The evolution equation for the running gauge coupling in the pure Yang-Mills theory has been computed in reference [1]. We use here mainly the lowest order result

$$\frac{\partial}{\partial t}\bar{g}_3^2 = \beta_{g^2} = -\frac{23\tau}{24\pi}\bar{g}_3^4(k)k^{-1} \tag{6}$$

where the deviation of τ from one accounts for the small contributions of scalar fluctuations which remain to be computed[2]. Furthermore, we need the anomalous dimension of the scalar field. For our purpose it can be approximated by [17]

$$\eta_\varphi = -\frac{\partial \ln Z_\varphi}{\partial t} = -\frac{1}{4\pi}\bar{g}_3^2(k)k^{-1}. \tag{7}$$

3 Running quartic coupling

A convenient quantity for an investigation of the effective potential is the ρ-dependent quartic coupling

$$\bar{\lambda}_{3,k}(\rho) = U_k''(\rho) = \frac{\partial^2 U_{3,k}}{\partial {\rho_3}^2}. \tag{8}$$

Knowing for $k = 0$ the function $\bar{\lambda}_3(\rho) = \bar{\lambda}_{3,0}(\rho)$, the high temperature effective potential $U(\rho) = U_0(\rho)$ can be reconstructed by integration and translation to a four dimensional normalization. One of the two integration constants is irrelevant and the other (the mass term linear in ρ) can be found by adapting $U(\rho)$ to the perturbative result for large ρ where the three dimensional running of the couplings is irrelevant. In fact, for large ρ such that $m_B^2(\rho) > k_T^2$ one may use the one loop potential [18]

$$\tilde{U}_3(\rho_3) = -\mu^2(T)\rho_3 + \frac{1}{2}\Big(\bar{\lambda}_3 + \Delta\bar{\lambda}_3\Big){\rho_3}^2 - \frac{1}{12\pi}\Big(6m_B^3 + 3m_E^3 + \bar{m}_1^3 + 3\bar{m}_2^3\Big) \tag{9}$$

with $\bar{m}_1^2 = 3\bar{\lambda}_3\rho_3 - \mu^2(T)$, $\bar{m}_2^2 = \bar{\lambda}_3\rho_3 - \mu^2(T)$, $Z_\varphi = 1$. Here

$$\Delta\bar{\lambda}_3 = \frac{3\bar{g}_3^4}{64\pi^2 T}\left(1 + \frac{\sqrt{6}+\sqrt{2}}{8}\frac{M_h^3}{M_w^3}\right) \tag{10}$$

with M_h and M_w the masses of the Higgs scalar and the gauge boson respectively is chosen such that $\tilde{U}_3''(8\pi^2T^2/\bar{g}_3^2(k_T)) = \bar{\lambda}_3$. Two loop effects and corrections

[2] For a suitable choice of wave function renormalization constants in the infrared cutoff for the gauge bosons the lowest order result becomes independent of the gauge parameter α and can therefore be used for the Landau gauge employed in this paper.

from integrating out A_0 may be included [16]. We use here the mass term $\mu^2(T)$ as given by

$$\frac{\mu^2(T)}{T^2} = \frac{1}{2}\frac{M_h^2}{T^2} - \frac{3\pi}{4}\alpha_w c - \frac{\pi}{4}\alpha_w \frac{M_h^2}{M_w^2} \tag{11}$$

where $\alpha_w = g_4^2(k_T)/4\pi$, the weak fine structure constant at the scale k_T. Here $c = 1 - \frac{m_D}{\pi T} + \Delta c$ includes effects from integrating out the A_0 mode. We use $\Delta c = 0$ but higher loop corrections or the effects from including the quark fluctuations can be accounted for by an appropriate nonvanishing Δc. For example including the top quark and using 6 quark flavours for the Debye mass yields $\Delta c = \frac{2M_{top}^2}{3M_w^2} + \frac{\sqrt{5}-\sqrt{11}}{\sqrt{6}}\frac{g_4}{\pi}$ where the second term accounts for the modification of m_D. The initial conditions for the flow equation described below will be expressed for fixed $\mu^2(T)/T^2$ and M_h^2/M_w^2. In consequence, $\Delta c \neq 0$ results in a simple rescaling of temperature and the scalar field according to

$$\begin{aligned} T_{mod}^{-2} &= T^{-2} + \frac{3\pi\alpha_w}{2M_h^2}\Delta c \\ \varphi_{mod}/\varphi &= T_{mod}/T. \end{aligned} \tag{12}$$

Here T_{mod} is appropriate for $\Delta c \neq 0$ whereas T represents the scaling used in this work for $\Delta c = 0$. The above simple rescaling property is very useful for a quantitative comparison with authors using different prescriptions for the effective three dimensional theory.

The evolution equation for the k-dependence of $\bar{\lambda}_3(\rho_3)$ can be infered from (2) by differentiating twice with respect to ρ_3 and reads

$$\frac{\partial \bar{\lambda}_{3,k}(\rho_3)}{\partial t} = \frac{3}{32\pi}\left(\frac{Z_{\varphi,k}^2 \bar{g}_{3,k}^4 k^2}{(k^2+m_B^2)^{3/2}} + \frac{6Z_{\varphi,k}^{-2}\bar{\lambda}_{3,k}^2(\rho_3)k^2}{(k^2+m_1^2)^{3/2}} + \frac{2Z_{\varphi,k}^{-2}\bar{\lambda}_{3,k}^2(\rho_3)k^2}{(k^2+m_2^2)^{3/2}}\right) \tag{13}$$

where we have neglected terms $\propto U_k^{(3)}(\rho_3)$ and $U_k^{(4)}(\rho_3)$. We propose in this paper an approximate solution of the flow equation for $\bar{\lambda}_3(\rho_3)$ for $k = 0$. It is based on the observation that the ρ_3-dependent mass terms m_B^2, m_1^2, and m_2^2 act in equation (2) as independent infrared cutoffs in just the same way as k^2. A variation of m^2 for $k^2 = 0$ is roughly equivalent to a variation of k^2 at $m^2 = 0$. We use this observation to translate the flow equation (13) into a renormalization group equation for $\bar{\lambda}_3(\rho_3)$ at $k = 0$: In equation (13) we replace $\frac{\partial}{\partial t}$ by $\frac{\partial}{\partial t'} = m_B\frac{\partial}{\partial m_B}$ and the factors $k^2\left(k^2+m^2\right)^{-3/2}$ by m^{-1}. In order to see that our simple prescription indeed corresponds to an approximate solution of the flow equation (13) we omit for a moment the two last terms in (13) which arise from the scalar fluctuations. Writing

$$\frac{\partial}{\partial t}\left(m_B\frac{\partial}{\partial m_B}\bar{\lambda}_{3,k}(\rho_3)\right) = \frac{3}{32\pi}Z_\varphi^2(k)\bar{g}_3^4(k)m_B^2\frac{\partial}{\partial t}\left(k^2+m_B^2\right)^{-3/2} \tag{14}$$

we observe that the right hand side is suppressed both for $k^2 \gg m_B^2$ and $k^2 \ll m_B^2$. Since the evolution of the quantity $m_B \frac{\partial}{\partial m_B} \bar{\lambda}_3$ is dominated by a narrow interval $k \simeq m_B$, we may approximate on the right hand side of equation (14) $\bar{g}_3^2(k)$ and $Z_\varphi(k)$ by $\bar{g}_3^2(m_B)$ and $Z_\varphi(m_B)$, and similar in the relation (3) between m_B^2 and ρ_3. Equation (14) is then easily integrated between $k = 0$ and $k = k_T$ to give

$$\begin{aligned} m_B \frac{\partial}{\partial m_B} \bar{\lambda}_{3,0}(\rho_3) &= \frac{3}{32\pi} Z_\varphi^2(m_B) \bar{g}_3^4(m_B) m_B^{-1} + m_B \frac{\partial}{\partial m_B} \bar{\lambda}_{3,k_T}(\rho_3) - \\ &\quad - \frac{3}{32\pi} Z_\varphi^2(m_B) \bar{g}_3^4(m_B) \frac{m_B^2}{\left(k_T^2 + m_B^2\right)^{3/2}}. \end{aligned} \tag{15}$$

The sum of the last two terms is small compared to the first term[3] which coincides exactly with our prescription. This type of arguments can be generalized for the scalar fluctuations. In summary, we can now work with a new effective infrared cutoff $k' = m_B$ which is a function of ρ_3 (we omit the prime on k in the following),

$$k^2 = m_B^2 = \frac{1}{2} Z_\varphi(k) \bar{g}_3^2(k) \rho_3. \tag{16}$$

This procedure transforms equation (13) into a simple differential equation for $\bar{\lambda}_3(\rho_3) = \bar{\lambda}_3(k(\rho_3))$. In terms of the renormalized coupling

$$\bar{\lambda}_R(k) = Z_\varphi^{-2}(k) \bar{\lambda}_3(k) \tag{17}$$

it reads

$$\frac{\partial}{\partial t} \bar{\lambda}_R(k) = \frac{3}{32\pi k} \left(\bar{g}_3^4(k) + \left(\sqrt{6} + \sqrt{2} \right) \bar{\lambda}_R^{3/2}(k) \bar{g}_3(k) \right) - \frac{1}{2\pi k} \bar{g}_3^2(k) \bar{\lambda}_R(k). \tag{18}$$

For the terms $\propto \frac{1}{m_1}$ and $\propto \frac{1}{m_2}$ from equation (15) we have approximated in (3) $U'(\rho_3) \simeq \rho_3 \bar{\lambda}_R(\rho_3)$ which amounts to neglecting the mass term. For negative $\bar{\lambda}_R(k)$ our approximation does not describe properly the effect of the scalar fluctuations. Since their contribution is small in this region we simply omit the terms $\propto \bar{\lambda}_R^{3/2}$ once $\bar{\lambda}_R(k)$ becomes negative.

The renormalization group equation (18) for the ρ_3-dependence of U'' is the central equation of this work. Except for the last term arising from the anomalous dimension it can be directly obtained by taking appropriate derivatives of the one loop formula (9), treating mass ratios such as m_B/m_1 as k-independent and replacing at the end the couplings $\bar{g}_3^2$ and $\bar{\lambda}_3$ by running couplings evaluated at the scale k. For $Z_\varphi = 1$ and $\bar{g}_3^2$, $\bar{\lambda}_3$ independent of k equation (18) reproduces exactly the one loop result. Our renormalization group equation enables us to

[3] This statement is immediately apparent for $m_B \ll k_T$ where both terms are seperately small. We expect it to hold also for $m_B \sim k_T$, but a proof needs a detailed understanding of the transition region between the effective three dimensional and the effective four dimensional theory.

include the effects of running couplings and the anomalous dimension. Combining equations (6), (8), (16), (17) and (18) we can compute the ρ_3-dependence of the high temperature effective potential by a solution of the flow equation. The initial values for this solution are set by equations (4), (11) and

$$\bar{\lambda}_3(k_T) = \frac{1}{4} g_4^2(k_T) T \frac{M_h^2}{M_w^2} - \frac{3 g_4^4(k_T) T^2}{64\pi m_D} + \Delta\bar{\lambda}_3 \tag{19}$$

where the last value is extracted from the validity of the one loop potential (9) at k_T.

4 Analytical approximations

Before turning to the numerical solution of the flow equations we display some analytical results in appropriate approximations.

First, from (6) one easily finds that the running gauge coupling is given by

$$\frac{1}{\bar{g}_3^2(k)} = \frac{1}{\bar{g}_3^2(k_T)} + \frac{23\tau}{24\pi}\left(\frac{1}{k_T} - \frac{1}{k}\right). \tag{20}$$

Thus, $\bar{g}_3^2(k)$ diverges as k approaches k_∞ with

$$k_\infty = \left(\frac{1}{k_T} + \frac{24\pi}{23\tau \bar{g}_3^2(k_T)}\right)^{-1}. \tag{21}$$

This reflects the well known fact that the $SU(2)$ Higgs model is confining in 3 dimensions. From (7) we can compute $Z_\varphi(k)$ and find

$$Z_\varphi(k) = \left(\frac{\bar{g}_3^2(k)}{\bar{g}_3^2(k_T)}\right)^{-\frac{6}{23\tau}}, \tag{22}$$

where we set $Z_\varphi(k_T) = 1$. Using (22) we can explicitly relate the renormalized to the unrenormalized couplings. Also, $\rho_3(k)$ is given by

$$\rho_3(k) = \frac{k^2}{2\pi\alpha_w T}\left(1 + \frac{23\tau\alpha_w}{12\pi}\left(1 - \frac{2\pi T}{k}\right)\right)^{1-\frac{6}{23\tau}}. \tag{23}$$

For small $\bar{\lambda}_R(k)$ we can neglect the term $\propto \bar{\lambda}_R^{3/2}$ on the right hand side of (18) and solve this equation analytically. One easily recovers the 1-loop result if one sets $\eta_\varphi = 0$ and $\bar{g}_3^2 = const.$. We can also find a solution if we include η_φ and the running of the gauge coupling. Defining

$$R(k) = \frac{\bar{\lambda}_R(k)}{\bar{g}_3^2(k)} \tag{24}$$

the flow equation reads

$$\frac{dR}{d\ln\bar{g}_3^2} = -\frac{9}{92\tau} - \left(1 - \frac{12}{23\tau}\right) R. \tag{25}$$

This is easily solved for R and one finds

$$\bar{\lambda}_R(k) = \left(\frac{\bar{g}_3^2(k)}{\bar{g}_3^2(k_T)}\right)^{\frac{12}{23\tau}} \bar{\lambda}_R(k_T) - \frac{9}{92\tau - 48}\bar{g}_3^2(k)\left(1 - \left(\frac{\bar{g}_3^2(k)}{\bar{g}_3^2(k_T)}\right)^{\frac{12}{23\tau}-1}\right). \tag{26}$$

The main changes as compared to the 1-loop calculations can be understood from the corresponding differential equations: The inclusion of η_φ lowers the scale at which U'' changes sign, whereas the running of the gauge coupling acts the opposite way. Thus at a given k, corresponding to a given ρ_3, the running of $\bar{g}_3^2$ makes the potential bend up less than the 1-loop calculation predicts. The inclusion of the neglected terms $\propto \bar{\lambda}_R^{3/2}$ will have the same effect as soon as they are not small, i.e. for larger Higgs masses.

In fig. 1 we have depicted the quartic coupling $U''(\rho)$ (in a four dimensional normalization) as a function of $\Phi = \rho_4^{1/2}$ for $M_h = 35$ GeV. The corrections due to the running gauge coupling and the anomalous dimension are small for $\Phi >$ 100 GeV. There are sizable modifications in the region 40 GeV $< \Phi <$ 60 GeV and large corrections for $\Phi <$ 40 GeV. Translated to the effective potential the running of $\bar{g}_3^2$ should strengthen the phase transition and lower the critical temperature. This is what one would naively expect, since the first order character of the transition is due to the gauge-boson loops. Thus, enhancing the coupling should give a transition more strongly first order. We should note, however, that the anomalous dimension has the opposite effect. To estimate the precise effects of these modifications on the shape of the potential we have to proceed to a numerical integration of equation (18).

5 Numerical solution of the flow equation

In order to make the numerical solution as easy as possible, we have transformed the system of differential equations (8) and (18) into a third order differential equation for U_3. Since equation (23) gives ρ_3 in terms of k and is not easily inverted analytically, we use k as the integration variable. This yields

$$\frac{\partial^3 U_3}{\partial k^3} = A^2 Z_\varphi^2 \beta^{(1)} + 3\frac{B}{A}\frac{\partial^2 U_3}{\partial k^2} - \left(3\frac{B^2}{A^2} - \frac{C}{A}\right)\frac{\partial U_3}{\partial k} \tag{27}$$

where

$$\begin{aligned}\beta^{(1)} &= \frac{3}{32\pi k^2}\left(\bar{g}_3^4(k) + \left(\sqrt{6}+\sqrt{2}\right)\bar{\lambda}_R^{3/2}(k)\bar{g}_3(k)\right)\\ A(k) &= \frac{\partial\rho_3}{\partial k}\ ;\ B(k) = \frac{\partial^2\rho_3}{\partial k^2}\ ;\ C(k) = \frac{\partial^3\rho_3}{\partial k^3}.\end{aligned} \tag{28}$$

As initial conditions we use

$$\frac{\partial^2 U_3}{\partial k^2}(k_T) = A^2(k_T)\bar{\lambda}_3(k_T) + B(k_T)\frac{\partial \tilde{U}_3}{\partial \rho_3}(k_T)$$
$$\frac{\partial U_3}{\partial k}(k_T) = A(k_T)\frac{\partial \tilde{U}_3}{\partial \rho_3}(k_T)\ ;\ U_3(k_T) = \tilde{U}_3(k_T)\ ;\ Z_\varphi(k_T) = 1. \tag{29}$$

$\tilde{U}_3$ represents the 1-loop potential (9) such that

$$\frac{\partial \tilde{U}_3}{\partial \rho_3}(k_T) = -\mu^2(T) + \left(\bar{\lambda}_3 + \Delta\bar{\lambda}_3\right)\frac{8\pi^2 T^2}{\bar{g}_3^2(k_T)} - \frac{9}{12}T\left(\bar{g}_3^2(k_T) + \left(\sqrt{6}+\sqrt{2}\right)\frac{\bar{\lambda}_3^{3/2}}{\bar{g}_3(k_T)}\right). \tag{30}$$

A similar set of equations relates the derivatives of the potential with respect to ρ_3 to the solution of (27). We integrate equation (27) with the help of the Runge-Kutta method and use for all numerical work $g_4 = 2/3$, $M_w = 80.6$ GeV, and $\tau = 1$.

In fig. 2 we show the effective potential as obtained with our method for different temperatures and for masses of the Higgs scalar of 35 and 80 GeV. In all the plots we use four dimensional quantities and plot $\Delta U = U(\Phi) - U(0)$. For $M_h = 35$ GeV (fig. 2a) the first two curves correspond to the critical temperature as given by the one loop approximation ($T = 97.50$ GeV) and the critical temperature obtained from our renormalization group improved approach ($T = 95.85$ GeV). Even though the critical temperature is not changed by much, the shape of the potential at a given temperature varies considerably. At the one loop critical temperature there remains not even a local minimum once renormalization group effects are included! We also find important quantitative differences for the size of the barrier at the critical temperature in both approaches. This effect becomes larger for higher values of the Higgs mass. For $M_h = 80$ GeV (fig. 2b) the critical temperatures (185.23 GeV for one loop, 184.25 GeV for RG-improvement) remain similar, but the shape of the potential differs strongly (even though this is difficult to see on the scale we use in fig. 2b). We have also indicated by a square the value of Φ where the dimensionless gauge coupling $g^2(k) = \bar{g}_3^2(k)/k$ becomes as large as 2π, and similarly, by the end of the solid line, where it reaches 4π. These points may be considered as an estimate for the limit of validity of our approximations. To the left of this region we have to deal with a strongly interacting gauge theory. Straightforward use of our approach in this region would yield the potential as indicated by the diamonds. We observe that our renormalization group improved effective potential can be formally extended to $\Phi = 0$: The confinement scale k_∞ corresponds to $\rho = 0$ since by equation (16) $\rho_3 \propto \bar{g}_3^{-2}(k)k^2$ and $\bar{g}_3^2(k_\infty) = \infty$. This explains the different qualitative behaviour as compared to [3].

In order to demonstrate that $g^2 \sim 2\pi - 4\pi$ indeed corresponds to the onset of the strong coupling regime we notice that $g^2(k) = 2\pi$ is reached at a scale

$k \sim 1.5 k_\infty$, which is already very close to the confinement scale (cf. eq. (20)). The anomalous dimension η_φ reaches the value -1 for $g^2(k) \sim 4\pi$ (cf. eq. (7)). Instead of the lowest order estimate for the running of $\bar{g}_3^2$ (6) we may also use the improved nonperturbative estimate of reference [1],

$$\frac{\partial \bar{g}_3^2(k)}{\partial t} = -\frac{23}{24\pi k}\left(\frac{1}{1-\frac{21}{48\pi}\bar{g}_3^2(k)k^{-1}}\right)\bar{g}_3^4(k). \tag{31}$$

Here the β-function diverges[4] for $g^2(k) = \frac{48}{21}\pi$, which is a value close to 2π. For the β-function (31) the confinement scale turns out higher and corresponds now to a nonzero value of Φ. We compare the results of the β-functions (6) and (31) for the effective potential in fig. 3, where we also display the one loop potential at the same temperature. The diamonds correspond to (31) and this curve ends once β_{g^2} diverges. For ease of comparison we have shifted all three curves to conicide at $\Phi = 100$ GeV. The temperature chosen is the critical temperature for $M_h = 80$ GeV as obtained by the renormalization group improved potential with the lowest order β-function (6). We emphasize that strong interaction phenomena cover here the whole region between the two minima. Any perturbative estimate of details of the potential as needed for calculations of bubble nucleation and for a treatment of the cosmological dynamics of the phase transition seems highly unreliable for Higgs masses of about 80 GeV or higher.

At this point we should mention that the renormalization group improvement has already extended considerably the range of Φ where a reliable computation is available: In the standard perturbative loop calculations the φ-dependence of the effective gauge coupling is usually not taken into account. Since the gauge-boson fluctuations are crucial for creating the barrier responsible for the first order transition, a change of $\bar{g}_3^2$ by a factor of two as compared to the perturbative value (which in our language corresponds to $\bar{g}_3^2(k_T)$) seems to be at the limit of what is tolerable for a perturbative estimate to be quantitatively correct. From (20) we find that $\bar{g}_3^2(k)/\bar{g}_3^2(k_T) = 2$ corresponds to a value of $\Phi = 0.55T$ (we have indicated this value by a cross on the curves in fig. 2). In contrast, the value where $g^2(k) = 2\pi$ (squares in fig. 2) corresponds to $\Phi_{np} = 0.28T$ which is smaller by a factor of two. Inspection of figures 1 and 2a suggests that even the range $\Phi > 0.55T$ for the validity of the loop expansion is overestimated and a more conservative estimate amounts to $\Phi \gtrsim T$.

6 Strong electroweak interactions

We finally turn to the region of strong interactions to the left of the solid line in fig. 2. We first observe that our computation of the potential has effectively

[4] This is, of course, not a physical effect; see the discussion in [1]

included only the quantum fluctuations with $q^2 > k_\infty^2$ since even for $\Phi = 0$ the infrared cutoff is given by k_∞. In consequence, the potential we have computed and shown in figures 2 and 3 corresponds to the average potential U_{k_∞} rather than to the effective potential U_0. For Φ sufficiently large, i.e. for $\Phi > \Phi_{np}$ to the right of the squares in fig. 2, the difference between U_0 and U_{k_∞} should be small since the contribution of the low momentum modes is suppressed by an effective infrared cutoff $m_B \gg k_\infty$. This is not true anymore in the region of small Φ where the low momentum fluctuations are expected to produce large nonperturbative effects. In particular, we notice that the ansatz (1) becomes insufficient: At the scale k_∞ the gauge boson kinetic term $\propto Z_F(k_\infty)$ vanishes $Z_F(k)$ and becomes negative [1] for $k < k_\infty$. This is a clear indication that for $k = 0$ the minimum of the Euclidian effective action does not occur for $F_{\mu\nu}F^{\mu\nu} = 0$ but rather for a nonzero value of F^2 [19]. One expects W-boson condensates in close analogy to the gluon condensates in QCD. The best way to visualize these effects in the context of the effective average action is perhaps the introduction of a composite scalar field Θ for the operator $\frac{1}{4}F_{\mu\nu}F^{\mu\nu}$. This can be done at a scale in the vincinity of (somewhat above) k_∞ according to the general formalism proposed in [20]. The average scalar potential is then generalized to a potential depending on two scalar degrees of freedom, $U_k(\Phi, \Theta)$. For $k > k_\infty$ the minimum of $U_k(\Phi, \Theta)$ occurs[5] at $<\Theta>= 0$ whereas for $k \to 0$ the minimum value $<\Theta>$ will be a nonvanishing function of Φ with $<\Theta>(\Phi) > 0$ for Φ smaller than some critical Φ_{cr}. In view of fig. 3 we may roughly associate the critical Φ_{cr} for the onset of condensation phenomena with Φ_{np}, denoted by the squares in fig 2. The W-boson condensate will lower the value of the effective potential $U(\Phi) = U(\Phi, <\Theta>(\Phi))$ in the region of small Φ as compared to the computed $U_{k_\infty}(\Phi, 0)$ [2]. We will present in the following some quantitative but rough estimates how this affects our picture of the phase transition.

Let us try to estimate the difference

$$\delta_1 = U_{k_\infty}(0,0) - U_0(0, <\Theta>(0)) \tag{32}$$

which measures how far the W-boson condensation lowers the potential at the origin. Since for $\Phi = 0$ the only relevant scale for the condensate is the confinement scale k_∞, we can infer from simple dimensional analysis

$$\Delta U_3 = K k_\infty^3 \tag{33}$$

with K a constant of order one. Since the running of the gauge coupling in three dimensions obeys a power law (in contrast to the four dimensional logarithms), the scale k_∞ is determined relatively precisely once the complete beta- function is known. In the relevant region the gauge coupling is large and there is no apparent

[5] Strictly speaking $<\Theta>$ may take a nonzero value depending on its precise definition. For the purpose of this qualitative discussion we shall speak of $<\Theta>= 0$ if the effect of $<\Theta>$ is small.

small dimensionless parameter in the problem and we will therefore use $K = 1$. With $k_\infty = 0.13T$ we infer for δ_1

$$\delta_1 = 2.2 \times 10^{-3} K T^4. \tag{34}$$

We have depicted δ_1 in figure 2 and also show the potential for the "nonperturbative critical temperature" corresponding to $T = 94.70$ GeV(173.74 GeV) for $M_h = 35$ GeV(80 GeV). For $M_h = 35$ GeV the change in the critical temperature is not very large, but the size of the barrier as obtained by extrapolating the potential from $\Phi = \Phi_{np}$ to the value $\Delta U = -\delta_1$ for $\Phi = 0$ is considerably enhanced by the W-boson condensation. For $M_h = 80$ GeV this effect is even more dramatic, and also the critical temperature is lowered considerably. A combination of our renormalization group improved potential for $\Phi > \Phi_{np}$ and other nonperturbative estimates of the critical temperatures using methods sensible to condensation phenomena - for example lattice calculations - can be used to determine the proportionality factor K. For this purpose we plot in figure 4 the critical temperature as a function of the Higgs-mass for various values of K. Here we have also included the (properly rescaled) results of recent lattice studies for $M_h = 35$ GeV [21] and 80 GeV [22] respectively. These values seem to support the general picture, yielding K of the order of 10. Conclusive evidence surely needs more data however.

It is also interesting to obtain an estimate for a lower bound on the critical temperature. For this purpose we use

$$\delta_2 = U_{k_\infty}(\Phi_{np}, 0) - U_0(0, <\Theta>\,(0)) = K' k_{np}^3 T \simeq 8 \times 10^{-3} K' T^4. \tag{35}$$

Since, as argued above, k_{np} denotes the scale for the onset of strong interaction phenomena it is difficult to conceive that the proportionality constant can exceed one by much. We display δ_2 for $K' = 1$ together with the potential for the corresponding critical temperature in fig. 2. The "lower bounds" on the critical temperature are

$$\begin{aligned} T_{cr} &> 92.54 \text{ GeV for } M_h = 35 \text{ GeV} \\ T_{cr} &> 159.14 \text{ GeV for } M_h = 80 \text{ GeV} \end{aligned} \tag{36}$$

and somewhat below these values for $K' > 1$. It is apparent from fig. 2 that the lower bounds on T_{cr} also correspond to upper bounds on the surface under the barrier which determines the strength of the first order phase transition. We observe that the use of the improved β-function (31) enhances k_∞ by a factor of two and leads to the guess $K = 8$. This yields T_{cr} in the vincinity of the "bound" (36), and seems to be favoured by the lattice results available.

Our estimates can be extended to larger values of the Higgs mass which are up to now difficult to access by alternative methods. In fig. 5 we plot the effective potential for $M_h = 140$ GeV and 200 GeV for three values of the temperature: The

upper curve corresponds to the critical temperature as determined from U_{k_∞} in the absence of condensation phenomena, the middle curve shows our estimate using $K = 1$ for the critical temperature including W-boson condensation, and the lower curve corresponds to the "lower bound" given above. For $M_h = 200$ GeV we notice that Φ_{np} (again indicated by a square) almost approaches the minimum of U for $T_{cr} = 318.9$ GeV. This may have important consequences for the dynamics of the phase transition: It is conceivable that there is almost no barrier between the minima at $\Phi = 0$ and $\Phi \neq 0$, and that the barrier is even completely absent for $M_h \gtrsim 200$ GeV. This could be interpreted as a change from a first order transition to an analytical crossover for very large Higgs masses [1]. Even though there is at presence no evidence for an analytical crossover, this possibility cannot be excluded for $M_h \gtrsim 200$ GeV!

7 Conclusions

In conclusion we have presented here a renormalization group improved estimate of the high temperature effective potential which determines the dynamics of the electroweak phase transition in the early universe. It is based on an approximative solution of an exact nonperturbative flow equation and includes properly several effects not accounted for in the presently available results from the loop expansion. This concerns, in particular, the running of the effective three dimensional gauge coupling and the anomalous dimension of the scalar field. We believe our estimates to be quantitatively accurate for large enough values of the scalar field, $\Phi > \Phi_{np}$. In this region of field space, the differences as compared to the loop expansion are already considerable even for a mass of the Higgs scalar as low as 35 GeV, being further enhanced for large scalar masses. We argue that nonperturbative effects not included in the present calculation further lower the critical temperature. They also enhance the barrier characteristic for the strength of the first order phase transition for low and moderate scalar masses ($M_h \lesssim 100$ GeV). This may lead to a sufficient strength of the first order transition to be compatible with electroweak baryogenesis for realistic masses of the Higgs scalar. For large scalar masses ($M_h > 200$ GeV) it is not excluded that the barrier disappears and the phase transition turns into an analytical crossover. We have also estimated lower bounds on the critical temperature including nonperturbative effects. The main uncertainty in the present calculation concerns the size of nonperturbative condensates (W-boson condensation), which determine the behaviour of the potential for small values of the field. In view of the extreme sensibility of tunneling rates to the height of the barrier and the crucial importance of nonperturbative phenomena for an estimate of this barrier, we believe that a quantitative understanding of the dynamics of the electroweak phase transition has to wait for a reliable treatment of condensation phenomena by nonperturbative methods.

Acknowledgement
The authors would like to thank W. Buchmüller and M. Shaposhnikov for fruitful discussions.

References

[1] M. Reuter, C. Wetterich, Nucl. Phys. **B408** (1993), 91; ibid. **B417** (1994), 181; M. Reuter, C. Wetterich, Preprint HD-THEP-93-41, to appear in Nucl. Phys. B.

[2] M. Shaposhnikov, Phys. Lett. **B316** (1993), 112.

[3] W. Buchmüller, Z. Fodor, Preprint DESY 94-045.

[4] Proceedings of the NATO-Advanced-Research Workshop "Electroweak Physics and the Early Universe", Sintra, Portugal 1994, to be published.

[5] Proceedings of the International Europhysics Conference, Marseille, France 1993.

[6] V. A. Kuzmin, V. A. Rubakov, M. Shaposhnikov, Phys. Lett. **B155** (1985), 36;
M. Shaposhnikov, Nucl. Phys. **B287** (1987), 757; ibid. **B299** (1988), 797.

[7] L. Dolan, R. Jackiw, Phys. Rev. **D9** (1974), 3320;
G. W. Anderson, L. J. Hall, Phys. Rev. **D45** (1992), 2685;
M. E. Carrington, Phys. Rev. **D45** (1992), 2933;
M. Dine, R. G. Leigh, P. Huet, A. D. Linde, D. Linde, Phys. Rev. **D46** (1992), 550;
P. Arnold, O. Espinosa, Phys. Rev. **D47** (1993), 3546;
W. Buchmüller, Z. Fodor, T. Helbig, D. Walliser, Preprint DESY 93-121, to appear in Ann. Phys.;
D. Bödeker, W. Buchmüller, Z. Fodor, T. Helbig, Preprint DESY 93-147, to appear in Nucl. Phys.;
P. Arnold, L. G. Yaffe, Preprint UW/PT-93-24;
Z. Fodor, A. Hebecker, Preprint DESY 94-025.

[8] N. Tetradis, C. Wetterich, Nucl. Phys. **B398** (1993), 659.

[9] See e.g. P. Arnold, O. Espinosa, Phys. Rev. **D47**(1993), 3546.

[10] See e.g. D. J. Amit, *Field Theory, the Renormalization Group, and Critical Phenomena*, World Scientific, 1984.

[11] S. Weinberg, Phys. Lett. **B91** (1980), 51;
T. Appelquist, R. Pisarski, Phys. Rev. **D23** (1982), 2305;
S. Nadkarni, Phys. Rev. **D27** (1983), 917;
N. P. Landsman, Nucl. Phys. **B322** (1989), 498;
A. Jakovác, K. Kajantie, A. Patkós, Preprint HU-TFT-94-01.

[12] D. O'Connor, C. R. Stephens, Nucl. Phys. **B360** (1991), 297; Preprint DIAS-STP-93-19;
D. O'Connor, C. R. Stephens, F. Freire, Mod. Phys. Lett. **A8** (1993), 1779; Preprint THU 92/37.

[13] S. Coleman, E. Weinberg, Phys. Rev. **D7** (1973), 1888.

[14] C. Wetterich, Nucl. Phys. **B352** (1991), 529; Z. Phys. **C60** (1993), 461.

[15] C. Wetterich, Phys. Lett. **B301** (1993), 90.

[16] K. Farakos, K. Kajantie, K. Rummukainen, M. Shaposhnikov, Preprint CERN-TH.6973/94.

[17] M. Reuter, C. Wetterich, Nucl. Phys. **B391** (1993), 147.

[18] D. A. Kirzhnitz, A. D. Linde, Phys. Lett. **B72** (1972), 471; JETP **40** (1974), 628; Ann. Phys. **101** (1976), 195;
S. Weinberg, Phys. Rev. **D9** (1974), 3357;
A. D. Linde, Nucl. Phys. **B216** (1983), 421; Rep. Prog. Phys. **47** (1984), 925.

[19] G. K. Savvidy, Phys. Lett. **71B** (1977), 133;
I. A. Batalin, S. G. Matinyan, G. K. Savvidy, Sov. J. Nucl. Phys. **26** (1977), 214;
S. G. Matinyan, G. K. Savvidy, Sov. J. Nucl. Phys. **25** (1977), 118; Nucl. Phys. **B134** (1978), 539;
W. Dittrich, M. Reuter, Phys. Lett. **128B** (1983), 321;
M. Reuter, C. Wetterich, Preprint HD-THEP-94-6, to appear in Phys. Lett. B.

[20] U. Ellwanger, C. Wetterich, Nucl. Phys. **B423** (1994), 137.

[21] K. Kajantie, K. Rummukainen, M. Shaposhnikov, Nucl. Phys. **B407** (1993), 356.

[22] K. Farakos, K. Kajantie, K. Rummukainen, M. Shaposhnikov, Preprint CERN-TH.7244/94.

Figure Caption

Fig. 1 Different approximations to the effective quartic scalar coupling for $M_h =$ 35 GeV Higgs at the RG-improved critical temperature.

Fig. 2 Renormalization group improved effective potential for $M_h = 35$ and 80 GeV at different temperatures.

Fig. 3 Comparison of the effective potential using different β-functions for the gauge coupling.

Fig. 4 Critical temperature including condensation effects as a function of the Higgs-mass for different values of K.

Fig. 5 Renormalization group improved effective potential for $M_h = 140$ and 200 GeV at different temperatures.

This figure "fig1-1.png" is available in "png" format from:

http://arXiv.org/ps/hep-ph/9409295v2

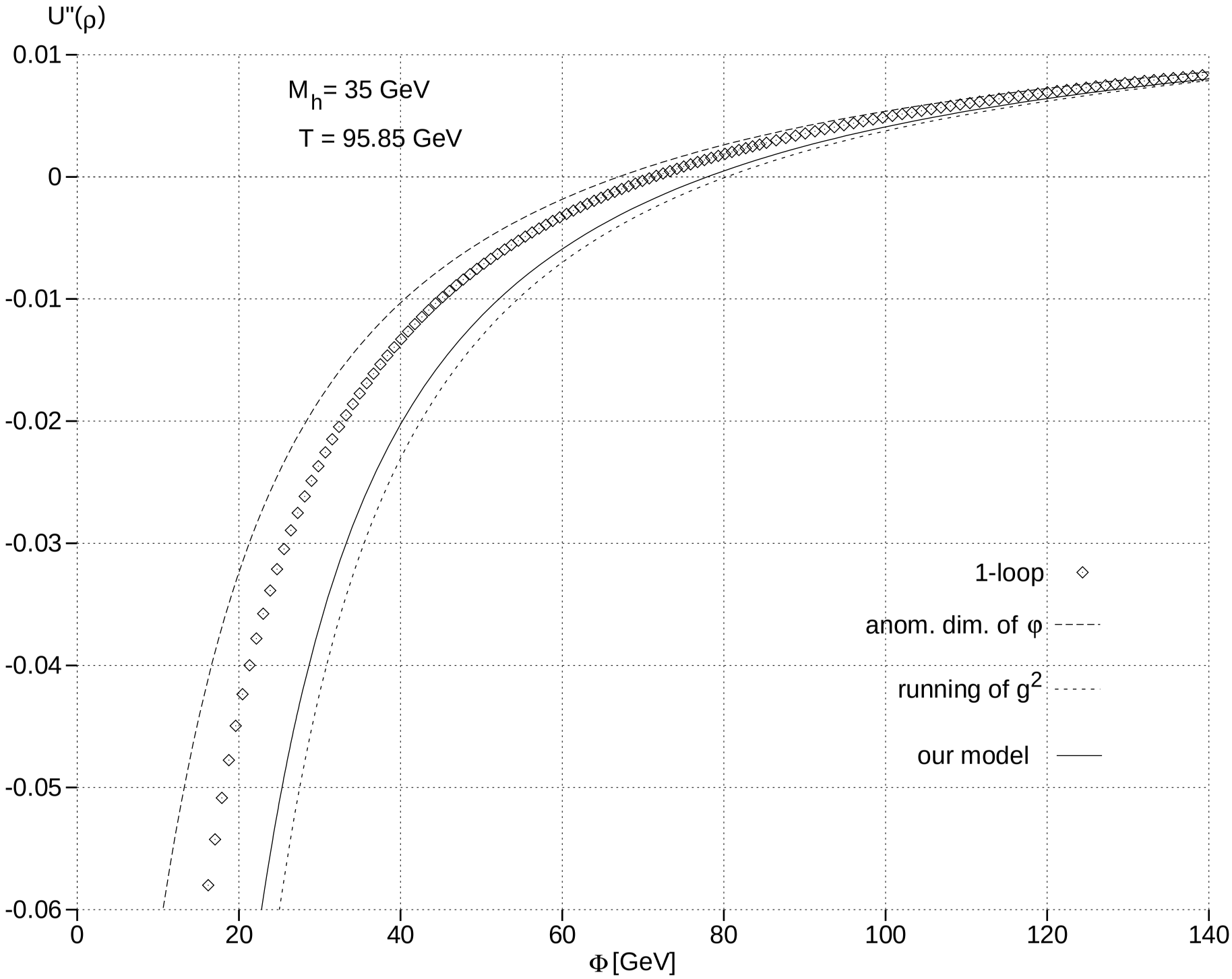
U"(ρ)
0.01
0
-0.01
-0.02
-0.03
-0.04
-0.05
-0.06
0
20
40
60
80
100
120
140
Φ [GeV]
M_h = 35 GeV
T = 95.85 GeV
1-loop
anom. dim. of φ
running of g^2
our model

This figure "fig2-1.png" is available in "png" format from:

http://arXiv.org/ps/hep-ph/9409295v2

This figure "fig1-2.png" is available in "png" format from:

http://arXiv.org/ps/hep-ph/9409295v2

This figure "fig2-2.png" is available in "png" format from:

http://arXiv.org/ps/hep-ph/9409295v2

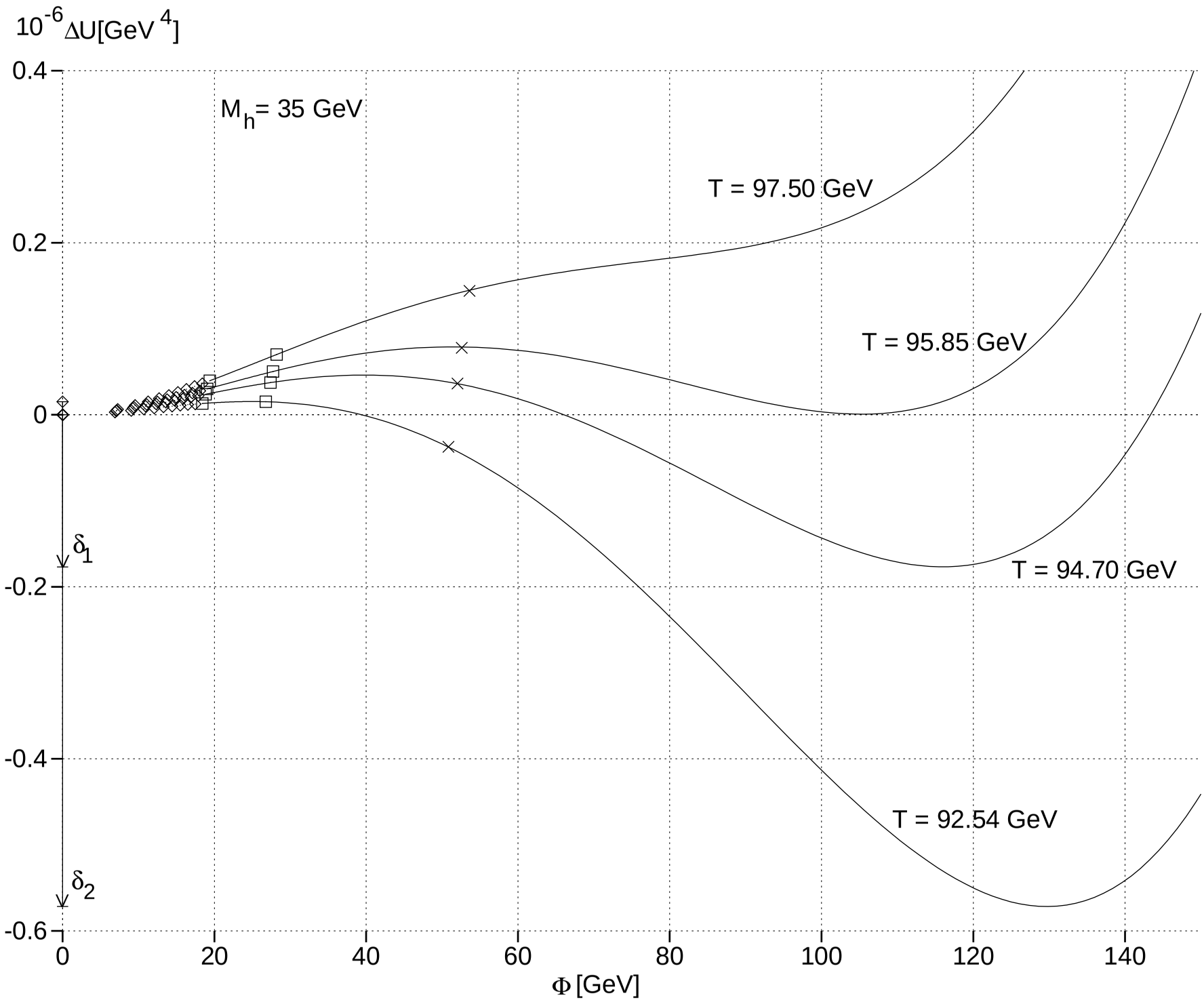
$10^{-6}\Delta U[GeV^4]$
0.4
0.2
0
-0.2
-0.4
-0.6
M_h= 35 GeV
T = 97.50 GeV
T = 95.85 GeV
T = 94.70 GeV
T = 92.54 GeV
δ_1
δ_2
0
20
40
60
80
100
120
140
Φ [GeV]

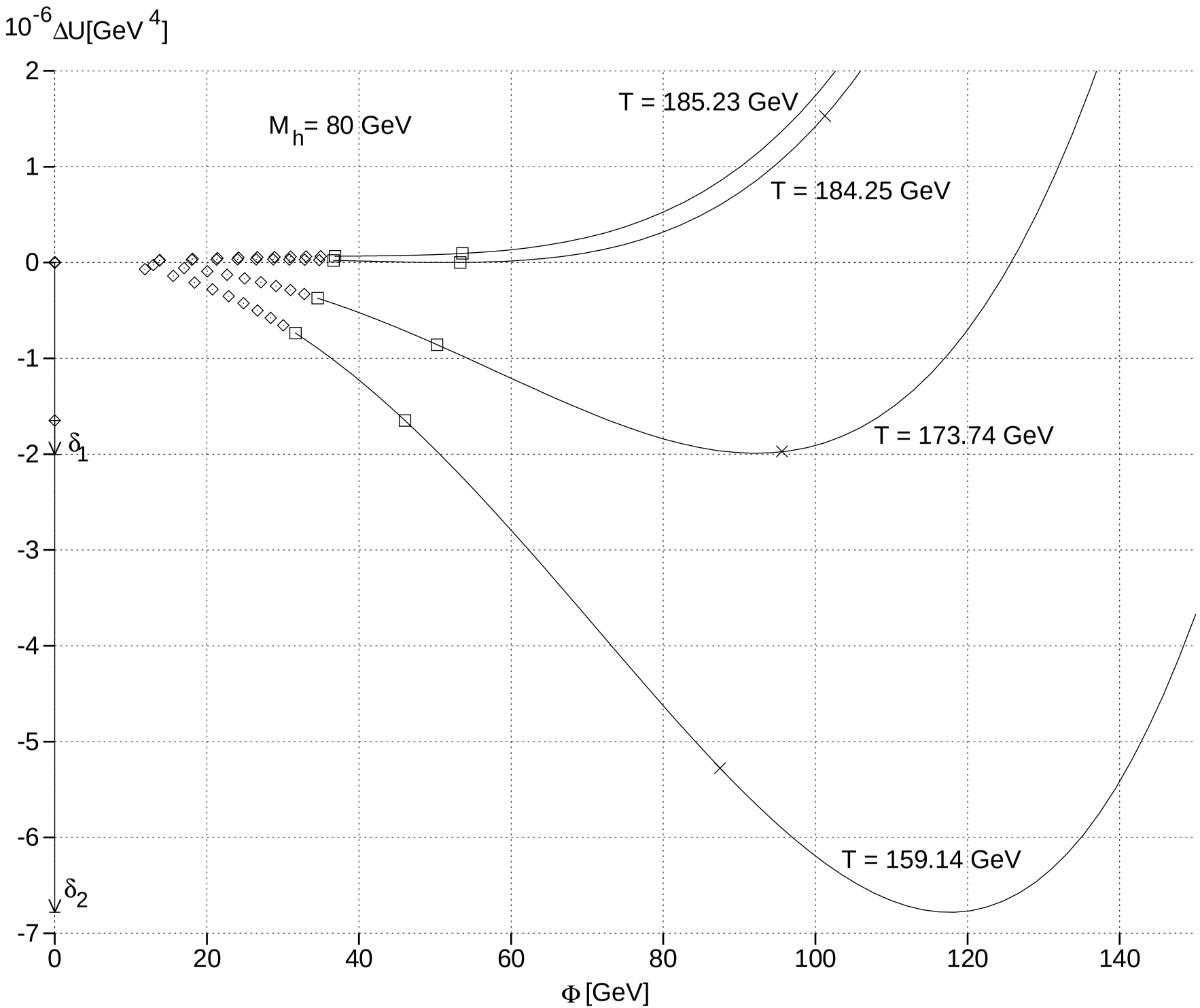
$10^{-6}\Delta U[\mathrm{GeV}^4]$
M_h= 80 GeV
T = 185.23 GeV
T = 184.25 GeV
T = 173.74 GeV
T = 159.14 GeV
δ_1
δ_2
2
1
0
-1
-2
-3
-4
-5
-6
-7
0
20
40
60
80
100
120
140
Φ [GeV]

This figure "fig1-3.png" is available in "png" format from:

http://arXiv.org/ps/hep-ph/9409295v2

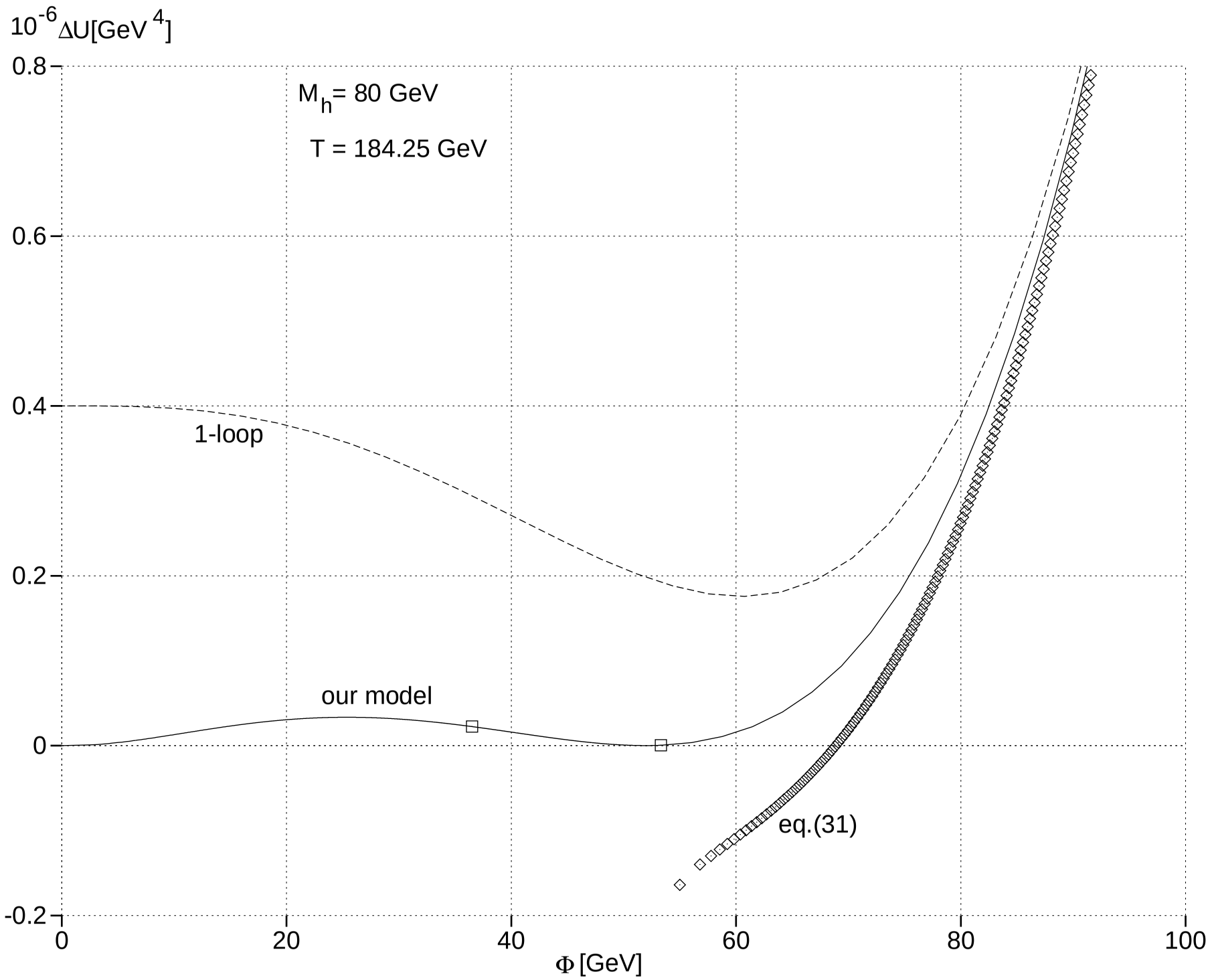
$10^{-6}\Delta U[\mathrm{GeV}^4]$
0.8
0.6
0.4
0.2
0
-0.2
M_h= 80 GeV
T = 184.25 GeV
1-loop
our model
eq.(31)
0
20
40
60
80
100
Φ [GeV]

This figure "fig1-4.png" is available in "png" format from:

http://arXiv.org/ps/hep-ph/9409295v2

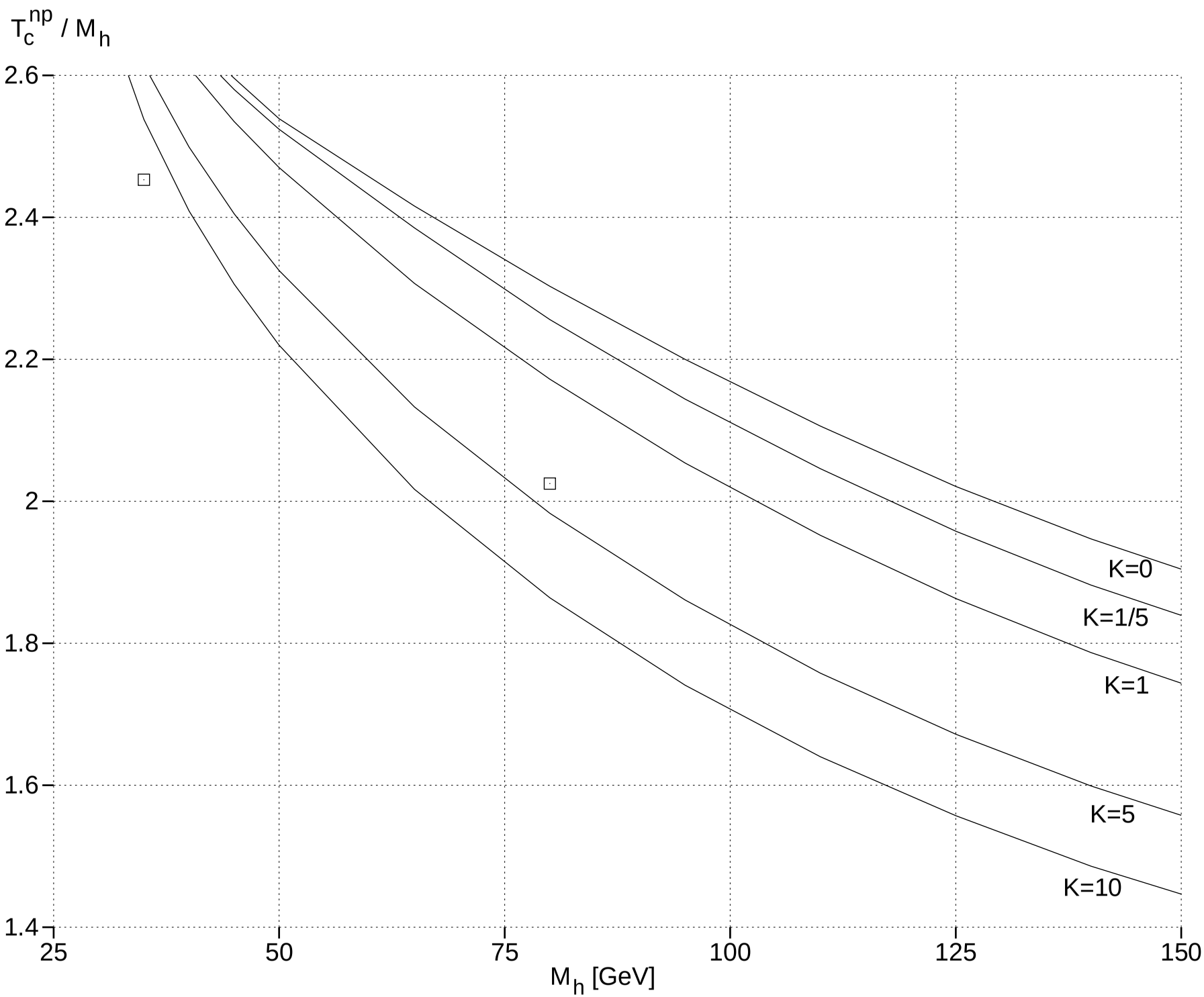
T_c^{np} / M_h
2.6
2.4
2.2
2
1.8
1.6
1.4
25
50
75
100
125
150
M_h [GeV]
K=0
K=1/5
K=1
K=5
K=10

This figure "fig1-5.png" is available in "png" format from:

http://arXiv.org/ps/hep-ph/9409295v2

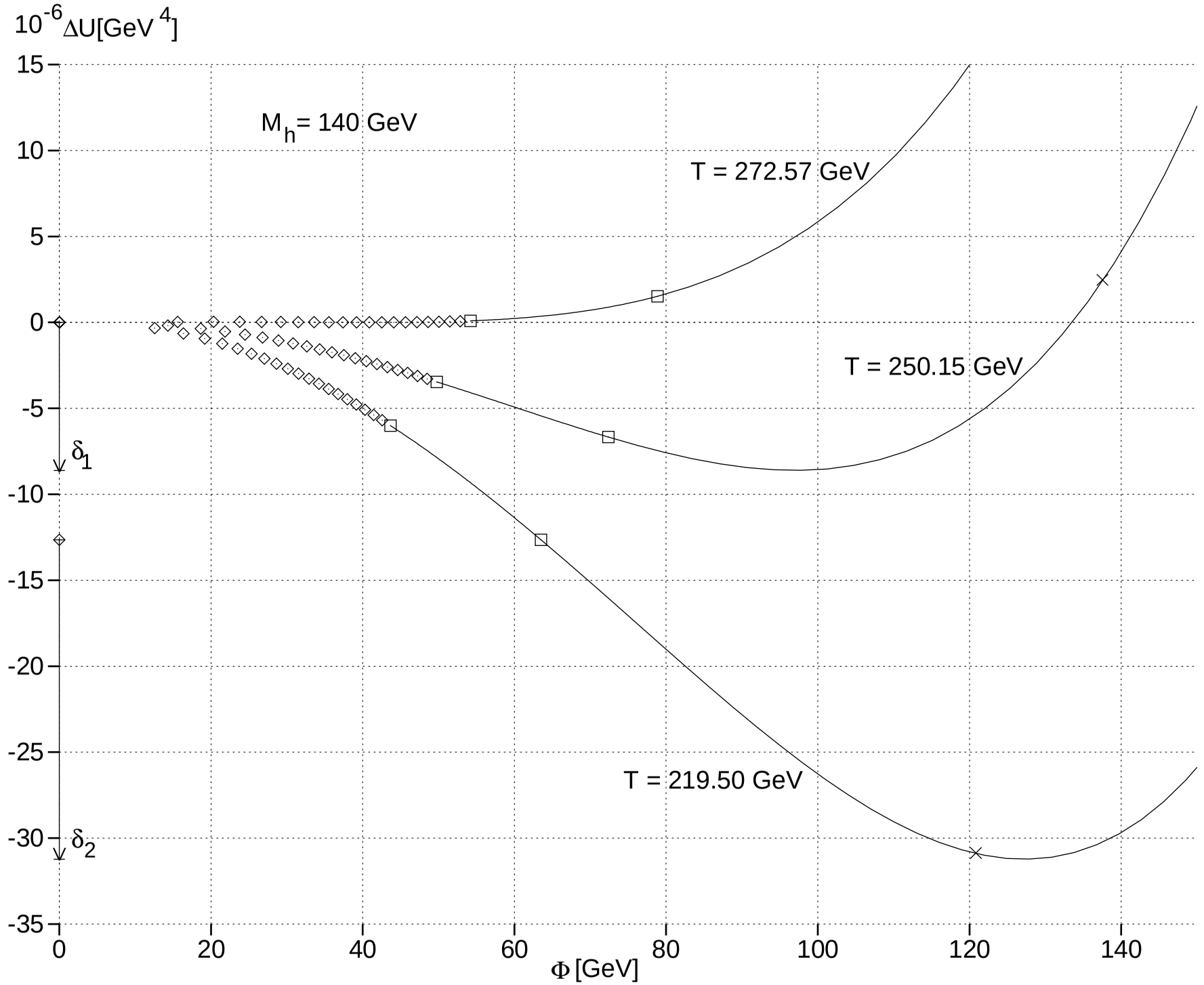
$10^{-6}\Delta U[GeV^4]$
15
10
5
0
-5
-10
-15
-20
-25
-30
-35
M_h= 140 GeV
T = 272.57 GeV
T = 250.15 GeV
T = 219.50 GeV
δ_1
δ_2
0
20
40
60
80
100
120
140
Φ [GeV]

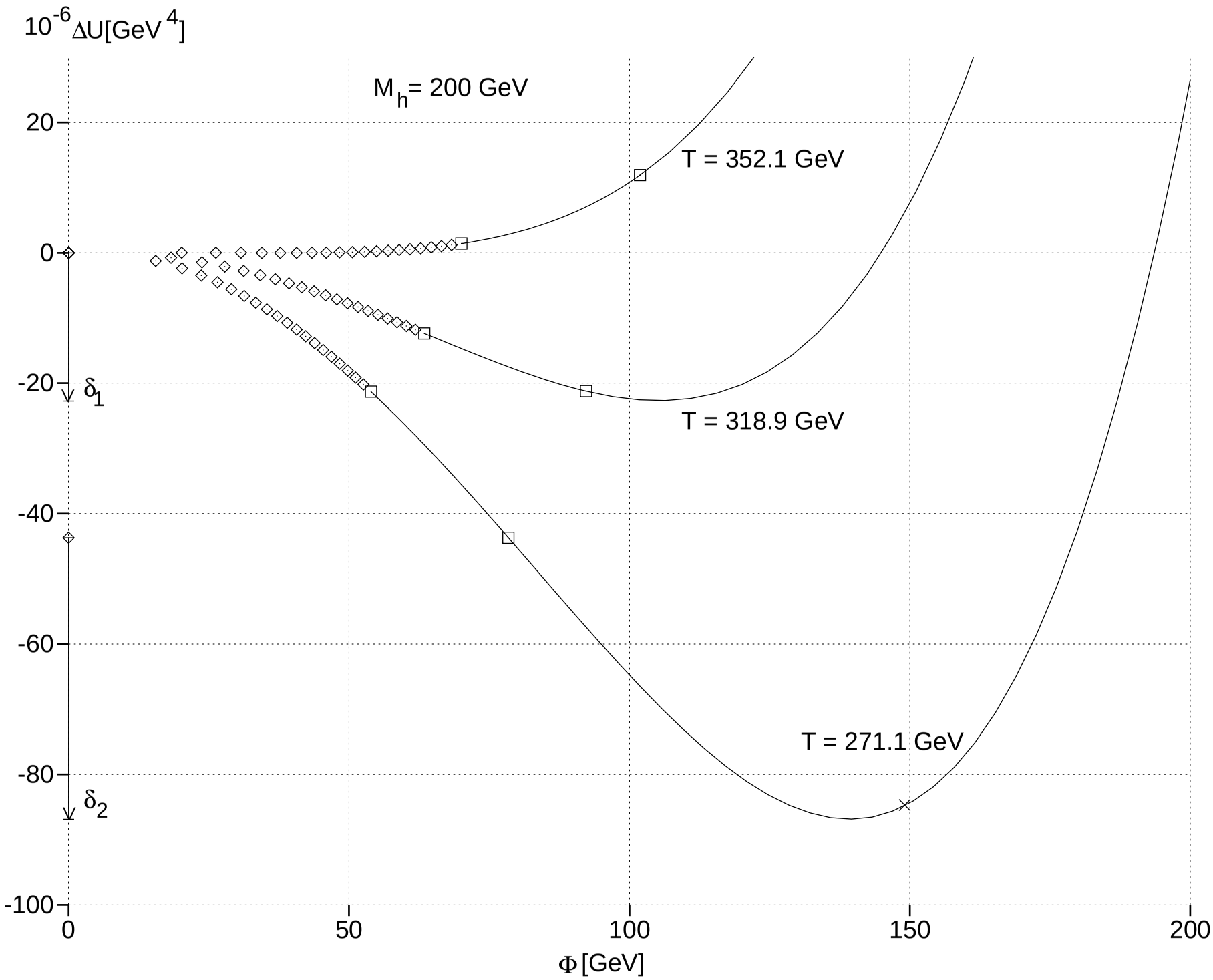
$10^{-6}\Delta U[GeV^4]$
M_h= 200 GeV
T = 352.1 GeV
T = 318.9 GeV
T = 271.1 GeV
δ_1
δ_2
20
0
-20
-40
-60
-80
-100
0
50
100
150
200
Φ [GeV]